 DOI: 10.1002/masy.200651034

Structural Phase Transitions of Aliphatic Nylons Viewed from the Simultaneous Measurements of WAXD and SAXS

Kohji Tashiro,[*1] *Kazuhiro Takeuchi,*[1] *Yasuaki Ohta,*[1] *Makoto Hanesaka,*[1] *Tomoko Hashida,*[2] *Yayoi Yoshioka,*[2] *Chellaswami Ramesh*[3]

Summary: Structural changes occurring in the high temperature region of doubly-oriented nylon 10/10 sample have been investigated through the temperature-dependent simultaneous measurements of wide-angle and small-angle X-ray scatterings, and the results were compared with the infrared spectral data as well as the molecular dynamics simulation results. In the Brill transition region of 150–180 °C the methylene segments are conformationally disordered with keeping the intermolecular hydrogen bonds. During this phase transition the stacked lamellar structure did not change very much: the lamellae are tilted by ca. 34° from the draw axis and the long period is almost 160 Å. In the temperature region immediately below the melting point the molecular chains were found to be contracted by ca. 10% the original repeating period and the intermolecular hydrogen bonds were almost broken, causing the violent rotational and translational motions of the chains around the chain axis. At the same time the long period increased remarkably from 160 Å to 410 Å and the originally tilted lamellae stood up in parallel to the draw axis.

Keywords: infrared spectra; nylon 10/10 brill transition; phase transition; small-angle X-ray scattering; wide-angle X-ray diffraction

Introduction

Aliphatic nylons are known to show the so-called Brill transition in a high temperature region below the melting point.[1] Though many papers were published so far about this transition,[2–29] the detailed structural changes had not yet been clarified enough satisfactorily. In a series of papers we investigated the temperature dependence of infrared spectra and X-ray diffraction patterns of nylon 10/10 and its model compounds, from which we have successfully clarified the essential features of the Brill transition phenomenon.[30–34] This successful deduction of concrete structural change can be made for the first time once a series of methylene progression bands observed in the infrared spectra were interpreted quantitatively. As shown in Figure 1, at room temperature the essentially planar-zigzag chains are connected with the strong intermolecular hydrogen bonds to form a sheet along the *a* axis. These sheets are stacked together by weaker van der Waals forces along the *b* axis. In the Brill transition region the planar-zigzag methylene parts are conformationally disordered but with keeping the intermolecular hydrogen bonds. The molecular dynamics calculation could reproduce this order-to-disorder phase transition quite reasonably. Recently we have found out an existence of a new phase transition in the temperature region above the Brill transi-

[1] Department of Future Industry-oriented Basic Science and Materials, Toyota Technological Institute, Tempaku, Nagoya 468-8511, Japan
Tel: (+81) 52 809 1790; Fax: (+81) 52 809 1721
E-mail: ktashiro@toyota-ti.ac.jp
[2] Osaka Technology Research Institute of Osaka Prefecture, Izumi, Osaka 594-1157, Japan
[3] Division of Polymer Science and Engineering, National Chemical Laboratory, Pune 411008, India

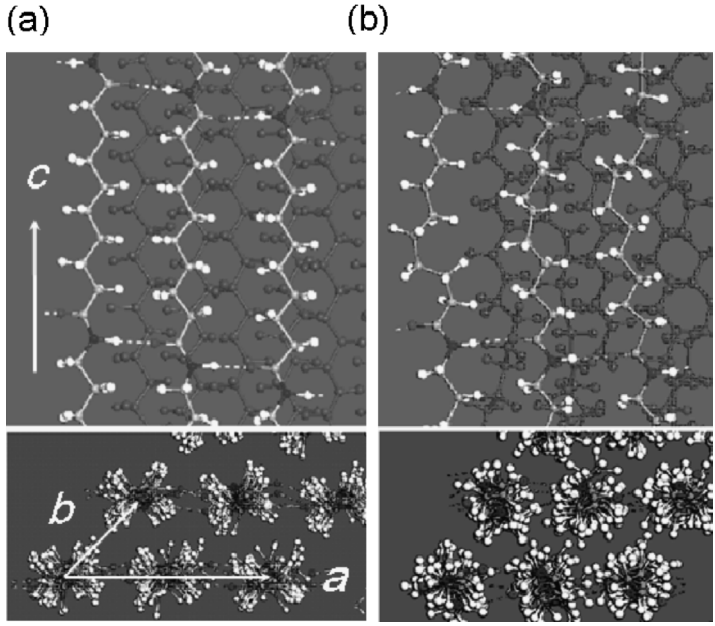

Figure 1.
Crystal structural change in Brill transition of nylon 10/10 deduced by molecular dynamics calculation.

tion or immediately below the melting point by performing the simultaneous measurement of wide-angle X-ray diffraction (WAXD) and small-angle X-ray scattering (SAXS) in the heating process of doubly-oriented nylon 10/10 sample. In the present paper we will review the structural study on the Brill transition phenomenon viewed from the points of WAXD and SAXS, and then describe the newly-detected phase transition occurring in the temperature region immediately below the melting point.

Experimental Section

Samples

Nylon 10/10 was kindly supplied by Shanghai Cellolose Works (Shanghaim China).

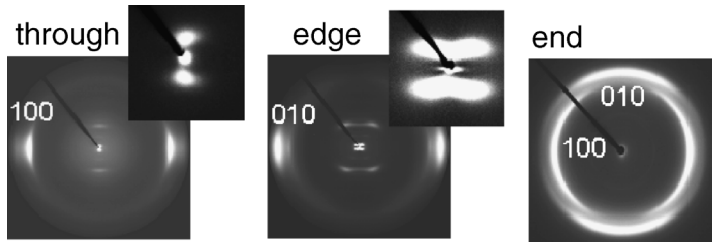

Figure 2.
WAXD and SAXS patterns taken at room temperature for the doubly-oriented nylon 10/10 sample. In the end pattern the rolled plane is parallel to the horizontal axis.

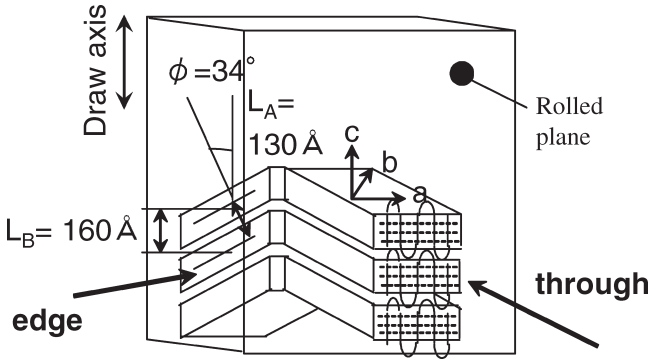

Figure 3.
Possible lamellar stacking structure of nylon 10/10 estimated from Figure 2.

The sample was melt-quenched into ice water bath and stretched above the hot plate about 5 times the original length. The thus-obtained uniaxially-oriented sample was rolled at room temperature to get the doubly-orineted sample.

Measurements:
The doubly-oriented sample was clamped with a metal holder and set into a home-made heater block. Temperature of the sample was monitored by a thermocouple attached to the sample directly. The temperature dependence of WAXD and SAXS was measured simultaneously using a 2- dimensional imaging plate system with a Cu-Kα line as an incident X-ray beam (MAC Science, DIP 1000), where the camera-to-detector distance was adjusted so that both of the WAXD and SAXS patterns could be taken on a sheet of imaging plate. The temperature depen-

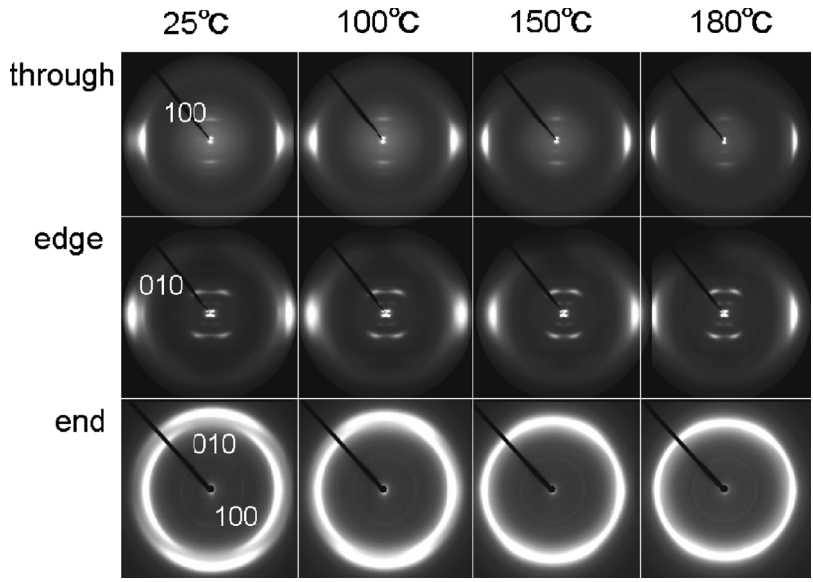

Figure 4.
Temperature dependence of wide-angle X-ray diffraction patterns taken for the doubly-oriented nylon 10/10 sample in the mutually perpendicular three directions.

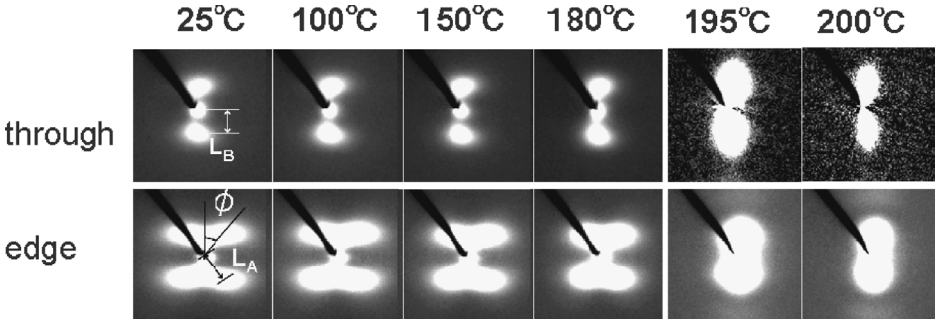

Figure 5.
Temperature dependence of small-angle X-ray scattering of doubly-oriented nylon 10/10 sample taken in the mutually-oriented two directions. The draw axis is along the vertical direction.

dence of infrared spectra of nylon 10/10 film was measured using a Varian FTS7000 Fourier-transform infrared spectrometer equipped with a home-made heater.

Results and Discussion

Lamellar Structure at Room Temperature

Figure 2 shows the WAXD and SAXS patterns taken for a doubly-oriented nylon 10/10 sample with the X-ray beam incident along the mutually perpendicular three directions. In the end pattern the 100 reflection is observed along the rolled plane. Correspondingly the 010 reflections are observed in the direction tilted by 20° from the normal to the rolled plane. Sometimes we get the doubly-oriented sample with the 010 reflection along the direction perpendicular to the rolled plane and the 100 reflections in the directions 20° tilted from the rolled plane. In this case the sheet planes are parallel to the rolled plane. In this way, depending sensitively on the sample preparation condition, nylon 10/10 shows sensitively the two different structures with the sheet planes parallel to or 20° tilted from the rolled plane. In the SAXS pattern, the 4-points scattering pattern is observed in the edge direction and the 2-points meridional scattering pattern in the through direction. The tilting angle estimated from the 4-points pattern is about 34°. As a result of the WAXD and SAXS measurements we can draw the lamellar stacking structure illustrated in Figure 3.

Temperature Dependence of WAXD and SAXS Patterns

The temperature dependence of WAXD patterns is shown in Figure 4. Figure 5 shows the case of SAXS patterns. In the end pattern, as the temperature is increased, the

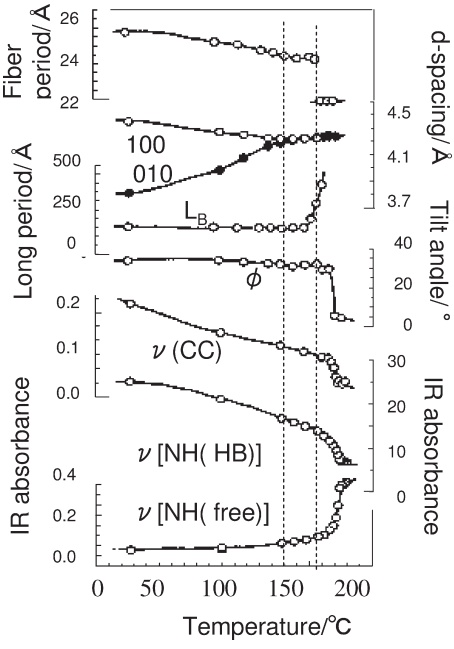

Figure 6.
Temperature dependence of various quantities evaluated for nylon 10/10 sample.

100 and 010 reflections shift and change into the 6 equi-distance reflections in every 60° different directions as shown in Figure 4, indicating the transformation from the triclinic to pseudo-hexagonal structure. The lattice spacings of these reflections are plotted against temperature as shown in Figure 6. The 4-points SAXS pattern changes gradually in the Brill transition region. The result of analysis of the SAXS patterns shown in Figure 5 is given also in Figure 6, where the tilting angle (ϕ) of the stacked lamellae decreases slightly and the long period (L_B) increases by about 10% the original value in the Briil transition region. The stacked lamellar structure estimated in the Brill transition region is illustrated in Figure 7(b). Contrast to the remarkable structural change in the crystal lattice, the lamellar stacking structure changes only slightly in this temperature region.

When the sample was heated furthermore and the temperature was increased beyond the Brill transition region, new meridional reflections were found to appear. Figure 8 shows the zoomed-up WAXD pattern in the low angle region, where the original meridional reflections decreased in intensity and the new reflections at higher angle side increased in intensity. Then the fiber period was found to be shortened from 24.9 Å in the Brill transition region to 22.5 Å at 185°C. At the same time the 4-points SAXS pattern changed to 2-points meridional scattering, indicating that the tilting of lamellae became zero (Figure 5). The long period was found to increase remarkably from 160 Å to 410 Å. All the experimental data are summarized in Figure 6, including the infrared spectral data. Above the Brill transition region, the fiber period is shortened by about 2.5 Å, suggesting the drastically activated thermal motion of the contracted chains with more highly disordered conformations. The lamellar stacking structure changes also remarkably: the lamellae of 400 Å period stand up vertically without any tilt as shown in Figure 7 (c). As detected in infrared spectral data the intermolecular hydrogen bonds become much weaker and the number of free NH groups increases. Therefore the transition observed in the temperature region immediately below the melting point is considered to be induced by the drastic translational and rotational motion of chains about the chain axis without any constraints by the intermolecular hydrogen bondings. This type of large structural change in the lamellar stacking mode is observed also in the ferroelectric phase transition of vinylidene fluoride-trifluoroethylene copolymers.[35] It should be noted here that the structural change observed in the higher temperature region had been predicted reasonably in our recently reported molecular dynamics calculation, where the chains are remarkably contracted because of the increase in the gauche content, and the intermolecular hydrogen bonds become much weaker.[34]

As for the mechanism of the newly-discovered phase transition, we might speculate that the original crystallites are melted and recrystallize into the different crystalline phase. However, the X-ray reflections

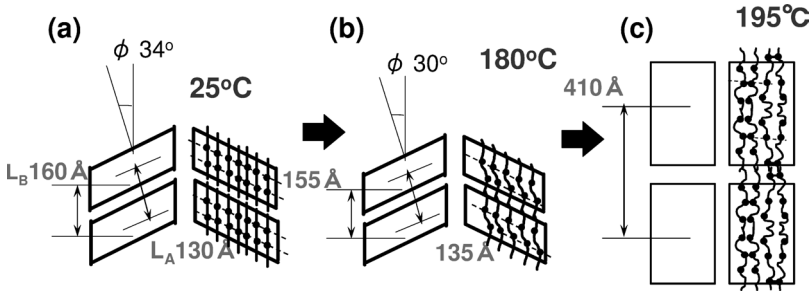

Figure 7.
Schematic illustration of the structural transformation in the heating process of nylon 10/10.

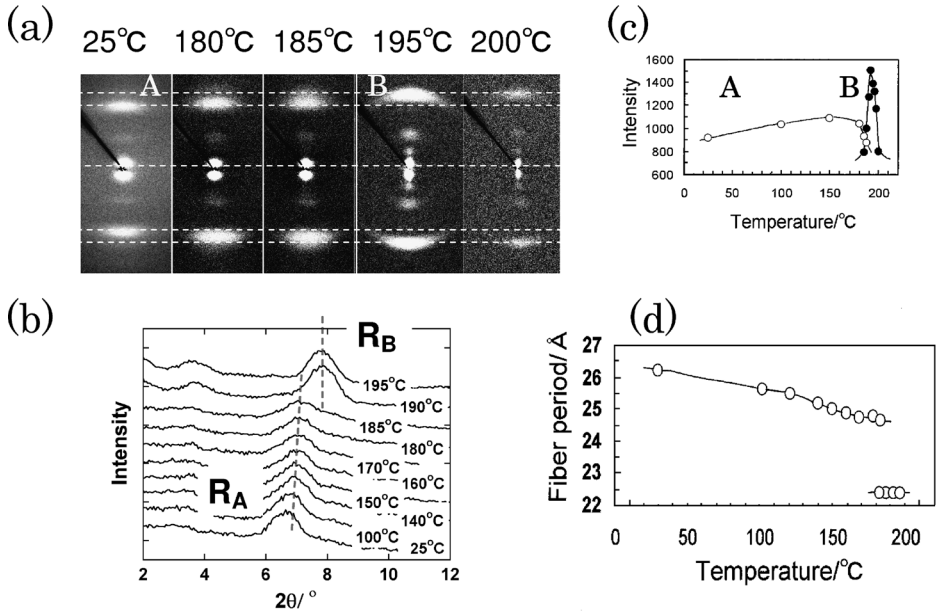

Figure 8.
(a) Temperature dependence of meridional reflections in the temperature region immediately below the melting point, (b) the profile change extracted from (a), (c) the intensity change of the meridional reflections A and B shown in (a), and (d) the change in fiber period.

of the two crystalline phases coexit in the transition region and the molecular chain orientation is kept almost perfectly in the actual observation. Therefore the observed transition may be assumed as the first-order solid-state transition. More detailed discussion will be reported in a near future.

Acknowledgements: This work was supported financially by the MEXT "Collaboration with Local Communities" Project (2005–2009)".

[1] Brill, R. J. *J. Prakt. Chem.* **1942**, *161*, 49.
[2] Itoh, T. *Jpn. J. Appl.Phys.* **1976**, *15*, 2295.
[3] Newman, B. A.; Sham, T. P.; Pae, K. D. *J. Appl. Phys.* **1977**, *48*, 4092.
[4] Newman, B. A.; Chen, P.; Pae, K. D.; Scheinbeim. *J. Appl. Phys.* **1980**, *51*, 5161.
[5] Starkweather, H. W., Jr.; Jones, G. A. *J. Polym.Sci., Polym. Phys. Ed.* **1981**, *19*, 467.
[6] Scheinbeim, J. I. *J. Appl. Phys.* **1981**, *52*, 5939.
[7] Kim K. G.; Newman, B. A.; Scheinbeim, J. I. *J. Polym.Sci., Polym. Phys. Ed.* **1985**, *23*, 2477.
[8] Biangardi, H. J. *J Macromol Sci, Phys.* **1990**, *B29*, 139.
[9] Murthy, N. S.; Curran, S. A.; Aharoni, S. M.; Minor H. *Macromolecules* **1991**, *24*, 3215.
[10] Radusch, H. J.; Stolp, M.; Androsch, R. *Polymer* **1994**, *35*, 3568.
[11] Ramesh, C.; Keller, A.; Eltink, S. J. E. A. *Polymer* **1994**, *35*, 2483.
[12] Jones, N. A.; Atkins, E. D. T.; Hill, M. J.; Cooper, S. J.; Franco, L. *Polymer* **1997**, *38*, 2689.
[13] Jones, N. A.; Cooper, S. J.; Atkins, E. D. T.; Hill, M. J.; Franco, L. *J. Polym. Sci., B: Polym. Phys.* **1997**, *35*, 675.
[14] Jones, N. A.; Atkins, E. D. T.; Hill, M. J.; Cooper, S. J.; Franco, L. *Macromolecules* **1997**, *30*, 3569.
[15] Cooper, S. J.; Atkins, E. D. T.; Hill, M. *J. Macromolecules* **1998**, *31*, 5032.
[16] Cooper, S. J.; Atkins, E. D. T.; Hill, M. *J. Macromolecules* **1998**, *31*, 8947.
[17] Cooper, S. J.; Atkins, E. D. T.; Hill, *J. Polym.Sci., B: Polym. Phys.* **1998**, *36*, 2849.
[18] Franco, L.; Cooper, S. J.; Atkins, E. D. T.; Hill, M. J.; Jones, N. A. *J. Polym. Sci., B: Polym. Phys.* **1998**, *36*, 1153.
[19] Murthy N. S.; Wang, Z.; Hisao, B. S. *Macromolecules* **1999**, *32*, 5594.
[20] Ramesh, C.; Gowd, E. B. *Macromolecules* **1999**, *32*, 3721.
[21] Jones, N. A.; Atkins, E. D. T.; Hill, M. J. *J Polym. Sci, B: Polym. Phys.* **2000**, *38*, 1209.

[22] Ramesh, C.; Gowd E. B. *Macromolecules* **2001**, *34*, 3308.
[23] Yang, X.; Li, G.; Zhou, E. *Macromol. Chem. Phys.* **2001**, *202*, 1637.
[24] Yang, X.; Tan, S.; Li, G.; Zhou, E. *Macromolecules* **2001**, *34*, 5936.
[25] Yan, D.; Li, Y. *Polymer* **2001**, *42*, 5055.
[26] Li, Y.; Yan, D.; Zhang, G. *J. Polym. Sci., B: Polym. Phys.* **2003**, *41*, 1422.
[27] Skrovanek, D. J.; Painter, P. C.; Colemen, M. M. *Macromolecules* **1986**, *19*, 699.
[28] Vasanthan, N.; Murthy, N. S.; Bray, R. G. *Macromolecules* **1998**, *31*, 8433.
[29] Cooper, S. J.; Coogan, M.; Everall, N.; Priestnall, I. *Polymer* **2001**, *42*, 10119.
[30] Yoshioka, Y.;Tashiro, K. *Polymer*, **2003**, *44*, 7007.
[31] Yoshioka, Y.;Tashiro, K.;C, Ramesh. *Polymer.* **2003**, *44*, 6407.
[32] Yoshioka, Y.;Tashiro, K. *J. Polym. Sci: part B: Polymer Physics.* **2003**, *41*, 1294.
[33] Tashiro, K; Yoshioka, Y. *Polymer.* **2004**, *45*, 6349
[34] Tashiro, K; Yoshioka, Y. *Polymer.* **2004**. *45*, 4337.
[35] Tashiro, K, *Mat. Res. Soc. Symp. Proc.* **2000**, *600*, 35.

